Japanese Journal of Applied Physics **50** (2011) 035101 **REGULAR PAPER**
DOI: 10.1143/JJAP.50.035101

Heterojunction Diodes Comprised of n-Type Silicon and p-Type Ultrananocrystalline Diamond/Hydrogenated Amorphous Carbon Composite

Shinya Ohmagari, Sausan Al-Riyami, and Tsuyoshi Yoshitake*

Department of Applied Science for Electronics and Materials, Kyushu University, Kasuga, Fukuoka 816-8580, Japan

Received September 24, 2010; accepted November 30, 2010; published online March 22, 2011

Heterojunction diodes comprised of p-type ultrananocrystalline diamond/hydrogenated amorphous carbon composite (UNCD/a-C:H) and n-type Si, wherein 3 at. % boron-doped UNCD/a-C:H films were deposited on Si substrates by pulsed laser deposition, were electrically studied. The current–voltage (I–V) characteristics showed the typical rectification action with a leakage current density of 4.7×10^{-5} A/cm^2 at a reverse voltage of -1 V. The carrier transport is expected to be in generation–recombination process accompanied by tunneling at low forward voltages of 0.1–0.5 V, and to be predominantly in tunneling at 0.5–1.0 V, from ideality factors estimated from the forward I–V curve. Grain boundaries in the UNCD/a-C:H film might act as centers for tunneling. From the capacitance–voltage measurement, the build-in potential of the heterojunction and an active carrier concentration in the p-type UNCD/a-C:H film were estimated to be 0.6 eV and 1.4×10^{17} cm^{-3}, respectively.

1. Introduction

Ultrananocrystalline diamond/hydrogenated amorphous carbon composite (UNCD/a-C:H) films, which are comprised of diamond crystallites with diameter of less than 10 nm embedded in an a-C:H matrix, have received considerable attention because of the following electrical and physical viewpoints. (a) They can be grown on foreign solid substrates.[1] (b) They possess higher temperature stability than that of diamond-like carbon (DLC). (c) They have unique optical and electrical properties owing to a large number of grain boundaries.[2,3] Here, the grain boundaries exactly means that the interfaces between UNCD crystallites and those between UNCD and an a-C:H matrix. For example, it has been experimentally reported that the UNCD/a-C:H films prepared by pulsed laser deposition (PLD)[4,5] and coaxial arc plasma deposition[6,7] possess large optical absorption coefficients of more than 10^5 cm^{-1} in the photon energy range between 3 and 6 eV, which might be due to grain boundaries.[8,9]

Also, the electrical properties of UNCD/a-C:H are unique as a semiconductor. It has been reported that nitrogen-doped UNCD/a-C:H films exhibit n-type conduction with an enhanced electrical conductivity.[10,11] So far it has been believed that the enhancement in the electrical conductivity is attributable to an increase in the sp^2 bonds in the film,[12,13] which probably lead to an increase in both the grain size and the grain boundary width. Theoretical calculations have predicted that nitrogen atoms are preferentially incorporated into grain boundaries,[14] and they increase the number of three-fold coordinated carbon atoms (sp^2 bonding) in the grain boundaries. As a result, a shift in the Fermi energy level toward the conduction band by approximately 0.4 eV takes place at a large nitrogen concentration. Concerning p-type UNCD/a-C:H, boron is a promising dopant element. For diamond and nanocrystalline diamond, boron atoms that substitutionally incorporated into diamond lattices forms an acceptor level with an activation energy of 0.38 eV above the valence band maximum of diamond. On the other hand, for boron-doped UNCD/a-C:H, it has been experimentally found that a large number of grain boundaries affect the formation of p-type conduction accompanied by an enhanced electrical conductivity[15] similarly to that of n-type conduction for nitrogen-doped UNCD/a-C:H. Both the n- and p-type conduction formations are specific to UNCD/a-C:H and they are quite different from those of diamond and a-C:H (so-called diamond-like carbon).

Semiconducting UNCD/a-C:H has recently received much attention because of not only the origins of the n- and p-type conduction being interesting from the physical viewpoint but also a new promising candidate applicable to electronic devices. Thus far, there have been few researches on the application to devices.[16,17]

We have realized p-type conduction with an enhanced electrical conductivity for boron-doped UNCD/a-C:H films prepared by PLD in our previous research.[15] In this study, heterojunction diodes comprised of p-type UNCD/a-C:H and n-type Si were fabricated. The electrical properties are discussed on the basis of the current–voltage (I–V) and capacitance–voltage (C–V) characteristics. The diodes showed a typical rectification behavior with a low leakage current. From the C–V measurement, the built-in potential of the heterojunction and the active carrier concentration in the UNCD/a-C:H film were estimated.

2. Experimental Procedure

Heterojunction diodes, wherein 3 at. % boron-doped UNCD/a-C:H films with a thickness of 100 nm were deposited on Si substrates at a substrate-temperature of 550 °C by PLD in the same manner as our previous study,[8] were prepared. The thickness and electrical resistivity of the n-type Si substrates were 260 μm and 1–5 Ω·cm, respectively. After the UNCD/a-C:H film deposition, Pd and Al electrodes were deposited on the p-type UNCD/a-C:H film and n-type Si substrate, respectively, by radio-frequency magnetron sputtering at room substrate temperature, and their ohmic contacts were confirmed.

From the X-ray photoemission spectra, the boron contents of the UNCD/a-C:H films were estimated.[15] The existence of UNCD crystallites was confirmed by powder X-ray diffraction (XRD) with 12 keV X-rays from synchrotron radiation at beamline 15 of the SAGA Light Source.[9] The I–V characteristics were evaluated at room temperature in the dark. The maximum bias voltage of an apparatus was ±100 V. As generally defined, the positive voltage applied to the p-type UNCD/a-C:H side is a forward bias. The C–V

*E-mail address: tsuyoshi_yoshitake@kyudai.jp

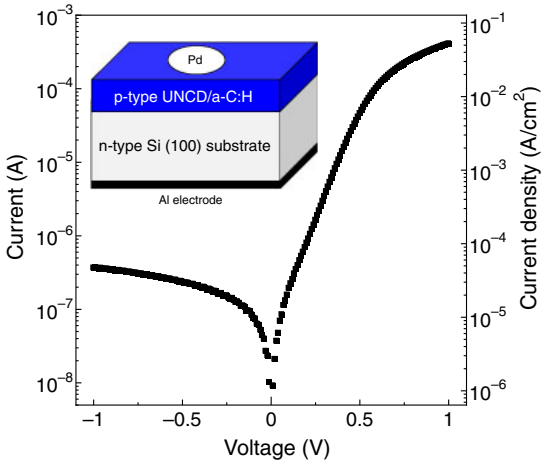

Fig. 1. (Color online) Current–voltage characteristics of a heterojunction diode comprised of p-type UNCD/a-C:H and n-type Si. The inset shows the schematic of the structure.

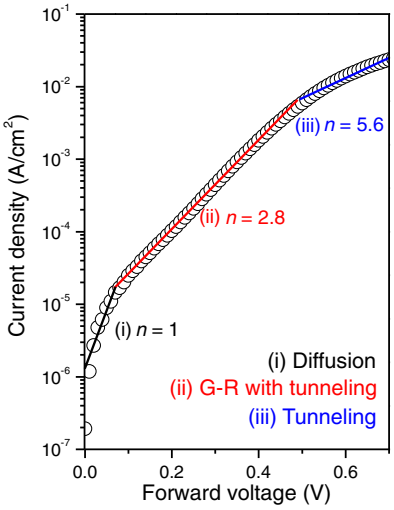

Fig. 2. (Color online) Current–voltage characteristics in the forward voltage range, which is magnified from the current–voltage curve as shown in Fig. 1. The ideality factor (n) is estimated to be 1, 2.8, and 5.6 for the regions (i), (ii), and (iii), respectively.

characteristics were measured at a signal frequency of 100 kHz with an applied AC bias of 50 mV.

3. Results and Discussion

At first, the UNCD/a-C:H films of the heterojunction diodes are briefly explained from the structural and electrical viewpoints. From the XRD pattern of 3 at. % boron-doped UNCD/a-C:H films, the existence of UNCD crystallites in the film was confirmed. Diffraction peaks due to graphite were not observed. From the van der Pauw measurement, the electrical conductivity of the 3 at. % doped UNCD/a-C:H film was estimated to be 0.14 $\Omega^{-1}\cdot$cm^{-1} at room temperature. The p-type conduction was confirmed thermally.

The I–V characteristics and the schematic of the heterojunction diode are shown in Fig. 1 and the inset, respectively. An active junction area was 7.8×10^{-3} cm^2. The I–V curve exhibited a typical rectification action with a rectification ratio of $\sim 10^3$ in the bias voltage range between -1 and 1 V. The boron-doped UNCD/a-C:H evidently acts as a p-type semiconductor. The leakage current at the reverse voltage of -1 V was 3.7×10^{-7} A, which corresponds to a current density of 4.7×10^{-5} A/cm^2. At reverse voltages greater than -1 V, the leakage current was exponentially increased with the reverse voltage. A breakdown behavior did not occur up to the maximum voltage (-100 V). The rectification ratio is extremely large as compared to those of heterojunction diodes comprised of p-type non-hydrogenated amorphous carbon (a-C) and n-type Si.[18,19] This might be predominantly owing to the enhanced electrical conductivity of UNCD/a-C:H by boron-doping.

Under low current injection, the effect of series resistance is negligible and the forward current can be expressed by

$$J = J_s \exp\left(\frac{qV}{nkT}\right). \quad (1)$$

Here, J, J_s, q, n, k, and T are the current density, saturation current density at zero bias, elementally electric charge, ideality factor, Boltzmann constant, and temperature, respectively. The values of the ideality factor theoretically become 1 and 2 for diffusion and generation–recombination processes, respectively.[20,21]

Figure 2 shows the magnification of the I–V curve in the forward voltage range. The forward current was divided into three regions. In the first region (i) at low bias voltages, the ideality factor was estimated to be 1.0. The diffusion current is dominant in the low bias region. In the region (ii), the ideality factor was estimated to be 2.8, and the saturation current density was interpolated to be 7.2×10^{-6} A/cm^2. The ideality factor value larger than 2 suggests that an additional process contributes to the conduction of carriers in addition to the generation–recombination (G–R) process ($n = 2$). The main origin of large ideality factors has been considered to be carrier tunneling in pn junctions.[22,23] In the UNCD/a-C:H film, the existence of a large number of grain boundaries is remarkably specific. They might act as centers for tunneling. In the region (iii), the ideality factor was estimated to be 5.6. This large value might imply that the tunneling effect become predominant.

The C–V curve of the diode is shown in Fig. 3. The capacitance at zero bias was estimated to be 22 nF/cm^2, and this value was decreased to be 8.3 nF/cm^2 at a reverse voltage of -5 V. The depletion region of the diode certainly spread under the reverse bias. The inset of Fig. 3 shows the $1/C^2$ plot versus reverse voltage. The build-in potential of the heterojunction was estimated to be 0.6 eV from the extended linear part of $1/C^2$ plot.

The active carrier concentration of the UNCD/a-C:H film was calculated using

$$\frac{1}{C^2} = \frac{2(\varepsilon_{Si}N_{Si} + \varepsilon_{UNCD}N_{UNCD})(V_{bi} - V)}{q\varepsilon_{Si}N_{Si}\varepsilon_{UNCD}N_{UNCD}}. \quad (2)$$

Here, ε_{UNCD}, ε_{Si} N_{UNCD}, N_{Si}, and V_{bi} are the dielectric constants of UNCD/a-C:H and Si, the carrier concentrations of the UNCD/a-C:H and Si, and the build-in potential of the heterojunction, respectively. The dielectric constants of diamond and a-C:H are 5.68 and 3.5, respectively from the previous reports.[24,25] The dielectric constant of UNCD/a-C:H should be close to those of diamond and a-C:H. On the assumption that the dielectric constant of UNCD/a-C:H is between those of diamond and a-C:H and the range of their

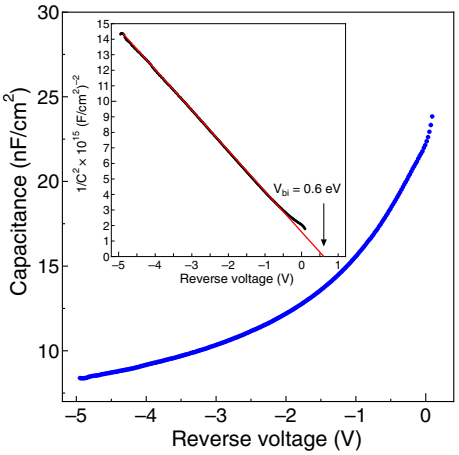

Fig. 3. (Color online) Capacitance–voltage characteristics of heterojunction diodes, measured at a signal frequency of 100 kHz. The inset shows the plot of $1/C^2$ versus reverse voltage.

difference is regarded as an error margin, the carrier concentration of the UNCD/a-C:H film was estimated to be $(1.4 \pm 0.3) \times 10^{17}\,\mathrm{cm}^{-3}$. Here, the carrier concentration of the Si substrate was $5 \times 10^{15}\,\mathrm{cm}^{-3}$. The depletion region width in the UNCD/a-C:H film can be calculated

$$W_{\mathrm{UNCD}} = \left[\frac{2N_{\mathrm{Si}}\varepsilon_{\mathrm{Si}}\varepsilon_{\mathrm{UNCD}}(V_{\mathrm{bi}} - V)}{qN_{\mathrm{UNCD}}(N_{\mathrm{Si}}\varepsilon_{\mathrm{Si}} + N_{\mathrm{UNCD}}\varepsilon_{\mathrm{UNCD}})}\right]^{1/2}. \quad (3)$$

Here, W_{UNCD} is the depletion region width in the UNCD/a-C:H film. The depletion region width was estimated to be 23 ± 5 and 43.5 ± 9.5 nm at the reverse voltages of -1 and -5 V, respectively. The depletion region certainly spreads toward the UNCD/a-C:H film. These values are more than a order of magnitude smaller than the widths (0.6 µm at -1 V and 1.2 µm at -5 V) of the depletion region that expands into the Si substrate. The depletion region can be flexibly controlled by changing the boron content in the UNCD/a-C:H film and selecting the carrier concentration of the Si substrates. We fabricated the diode and experimentally proved that boron-doped UNCD/a-C:H is applicable to a p-type semiconducting layer in diodes.

4. Conclusions

Heterojunction diodes comprised of p-type ultrananocrystalline diamond/hydrogenated amorphous carbon composite (UNCD/a-C:H) and n-type Si, wherein boron-doped UNCD/a-C:H films were deposited on Si substrates by pulsed laser deposition with boron-doped graphite targets were electrically investigated. The current–voltage (I–V) characteristics of the diodes showed that the typical rectification action with a high rectification ratio of $\sim 10^3$ between bias voltages of -1 and 1 V. From the estimation of ideality factor in forward characteristics, the current region was divided into three process: (i) diffusion current region under a low injection, (ii) generation–recombination accompanied with tunneling at 0.1–0.5 V, and (iii) dominant transport in tunneling current at 0.5–1.0 V. This implies that grain boundaries in the UNCD/a-C:H film might act as centers for tunneling. In the capacitance–voltage measurement, the build-in potential of heterojunction and the active carrier concentration in UNCD/a-C:H films were estimated to be 0.6 eV and approximately $1.4 \times 10^{17}\,\mathrm{cm}^{-3}$, respectively. The depletion region width in the UNCD:a-C/H film certainly spread with the reverse bias voltage.

Acknowledgements

The XRD and X-ray photoemission spectroscopic measurements were supported by Nanotechnology Network Japan (Kyushu Synchrotron Light Research Center, Proposal Nos. 090423N, 090662N, and 100320AS). The authors would like to express their deep gratitude to Dr. R. Ohtani, Dr. H. Setoyama, Dr. K. Sumitani, and Dr. E. Kobayashi, for their kind support in the measurement of XRD and X-ray photoemission spectra. The first author S.O. is supported by Research fellowship of the Japan Society for the Promotion of Science (JSPS) for Young Scientists.

1) A. R. Krauss, O. Auciello, D. M. Gruen, A. Jayatissa, A. Sumant, J. Tucek, D. C. Mancini, N. Moldovan, A. Erdemir, D. Ersoy, M. N. Gardos, H. G. Busmann, E. M. Meyer, and M. Q. Ding: Diamond Relat. Mater. **10** (2001) 1952.
2) W. Kulisch, C. Popov, E. Lefterova, S. Bliznakov, J. P. Reithmaier, and F. Rossi: Diamond Relat. Mater. **19** (2010) 449.
3) A. I. Shames, A. M. Panich, S. Porro, M. Rovere, S. Musso, A. Tagliaferro, M. V. Baidakova, V. Y. Osipov, A. Y. Vul', T. Enoki, M. Takahashi, E. Osawa, O. A. Williams, P. Bruno, and D. M. Gruen: Diamond Relat. Mater. **16** (2007) 1806.
4) K. Hanada, T. Nishiyama, T. Yoshitake, and K. Nagayama: J. Nanomater. **2009** (2009) 901241.
5) T. Yoshitake, A. Nagano, S. Ohmagari, M. Itakura, N. Kuwano, R. Ohtani, H. Setoyama, E. Kobayashi, and K. Nagayama: Jpn. J. Appl. Phys. **48** (2009) 020222.
6) K. Hanada, T. Yoshitake, T. Nishiyama, and K. Nagayama: Jpn. J. Appl. Phys. **49** (2010) 08JF09.
7) K. Hanada, T. Yoshida, Y. Nakagawa, and T. Yoshitake: Jpn. J. Appl. Phys. **49** (2010) 125503.
8) T. Yoshitake, A. Nagano, M. Itakura, N. Kuwano, T. Hara, and K. Nagayama: Jpn. J. Appl. Phys. **46** (2007) L936.
9) T. Yoshitake, Y. Nakagawa, A. Nagano, R. Ohtani, H. Setoyama, E. Kobayashi, K. Sumitani, Y. Agawa, and K. Nagayama: Jpn. J. Appl. Phys. **49** (2010) 015503.
10) S. Bhattacharyya, O. Auciello, J. Birrell, J. A. Carlisle, L. A. Curtiss, A. N. Goyette, D. M. Gruen, A. R. Krauss, J. Schlueter, A. Sumant, and P. Zapol: Appl. Phys. Lett. **79** (2001) 1441.
11) S. Al-Riyami, S. Ohmagari, and T. Yoshitake: Appl. Phys. Express **3** (2010) 115102.
12) J. Birrell, J. E. Gerbi, O. Auciello, J. M. Gibson, D. M. Gruen, and J. A. Carlisle: J. Appl. Phys. **93** (2003) 5656.
13) O. A. Williams, M. Nesladek, M. Daenen, S. Michaelson, A. Hoffman, E. Osawa, K. Haenen, and R. B. Jackman: Diamond Relat. Mater. **17** (2008) 1080.
14) P. Zapol, M. Sternberg, L. A. Curtiss, T. Frauenhein, and D. M. Gruen: Phys. Rev. B **65** (2001) 045403.
15) S. Ohmagari, T. Yoshitake, A. Nagano, R. Ohtani, H. Setoyama, E. Kobayashi, T. Hara, and K. Nagayama: Jpn. J. Appl. Phys. **49** (2010) 031302.
16) T. Zimmermann, M. Kubovic, A. Denisenko, K. Janischowsky, O. A. Williams, D. M. Gruen, and E. Kohn: Diamond Relat. Mater. **14** (2005) 416.
17) T. Zimmermann, K. Janischowsky, A. Denisenko, F. J. Hernández Guillén, M. Kubovic, D. M. Gruen, and E. Kohn: Diamond Relat. Mater. **15** (2006) 203.
18) X. Tian, M. Rusop, Y. Hayashi, T. Soga, T. Jimbo, and M. Umeno: Jpn. J. Appl. Phys. **41** (2002) L970.
19) S. S. Yap, H. K. Yow, and T. Y. Tou: Thin Solid Films **517** (2009) 5569.
20) W. Shockley: Bell Syst. Tech. J. **28** (1949) 435.
21) C. T. Sah, R. N. Noyce, and W. Shockley: Proc. IRE **45** (1957) 1228.
22) D. J. Dumin and G. L. Pearson: J. Appl. Phys. **36** (1965) 3418.
23) K. Mayes, A. Yasan, R. McClintock, D. Shiell, S. R. Darvish, P. Kung, and M. Razeghi: Appl. Phys. Lett. **84** (2004) 1046.
24) A. Grill: Thin Solid Films **355** (1999) 189.
25) M. Guerino, M. Massi, and R. D. Mansano: Microelectron. J. **38** (2007) 915.